ISSN 1070-3632, Russian Journal of General Chemistry, 2013, Vol. 83, No. 10, pp. 1823–1839. © Pleiades Publishing, Ltd., 2013.
Original Russian Text © R.V. Tsyshevsky, B. Nguen Van, A.G. Shamov, G.M. Khrapovskii, 2013, published in Zhurnal Obshchei Khimii, 2013, Vol. 83, No. 10, pp. 1611–1629.

Study of Geometry and Electronic Structure of Molecules, Cation-Radicals, and Anion-Radicals of Nitromethane, Dimethylnitramine, and Ethyl Nitrate

R. V. Tsyshevsky, B. Nguen Van, A. G. Shamov, and G. M. Khrapovskii

Kazan National Research Technologic University, ul. K. Marksa 68, Kazan, Tatarstan, 420015 Russia
e-mail: rtsyshev@gmail.com

Received July 30, 2012

Abstract—The geometry of cation-radicals and anion-radicals of nitromethane, dimethylnitramine, and ethyl nitrate have been computed by means of modern quantum-chemical methods. Their electron affinities and ionization potentials have been determined. The validity of the results has been confirmed by comparison with the experiment.

DOI: 10.1134/S107036321310006X

Nitrocompounds reactivity and its relation to the molecular structure has been a subject of many experimental [1–12] and theoretical [12–21] studies. To a great extent, this is connected with the design of highly efficient energetic materials and explosives with desired properties. Recently, the interest grew to the investigation of the decay mechanism of optically excited [22–25] and ionized [26–37] nitrocompounds. The study of the excited states are important in the context of direct optical initiation of explosives with no initiating additives, the latter being often shock- and heat-sensitive [38]. The mechanism and kinetics of the ionized molecules decomposition are of interest for development of the highly sensitive analyzers capable of detection of the finest particles of explosives, and also to separate them from the composition of the other nitro compounds by means of mass-spectrometry [32–37, 39, 40]. Reliable identification of explosives is a topical issue in the modern world due to the danger of terrorism. From the above-written it is clear that the information on the decay mechanism of anion-radicals and cation-radicals of simple compounds, models of explosives, is necessary to reliably identify individual explosives and their compositions based on their fragmentation products. The task is not trivial, firstly, due to differences in mechanism and kinetics of decay of neutral and ionized molecules [41–44]. The experimental determination of the kinetic parameters of the major decay stages is complicated in the case of ionized molecules of explosives. However, this information can be obtained applying the quantum-chemical methods.

Modern quantum-chemical methods are efficiently applied to determine the geometry and electronic structure of the explosives molecules, as well as to deduce the structure-reactivity relationship. The most popular approaches are hybrid methods of the density functional theory that have proved themselves reliable in studies of the reaction mechanisms of neutral molecules, being at the same time advantageous over the ab initio methods due to the relatively low requirements of the computational resources [16, 45]. However, in [46, 47] significant differences have been revealed in the mechanism of the gas-phase decay of butane cation-radical, as calculated by B3LYP and MP2 methods.

Thus, the proper choice of reliable quantum-chemical method to study the elementary stages of the ionized nitrocompounds decay has become of primary importance.

We applied various quantum-chemical methods to compute geometry parameters, atomic charges, ionization potentials, and electron affinities of simplest representatives of the explosive compounds class. The following model compounds were chosen: nitromethane (C-nitrocompound), ethyl nitrate (O-nitrocompound), and dimethylnitramine (N-nitrocompound).

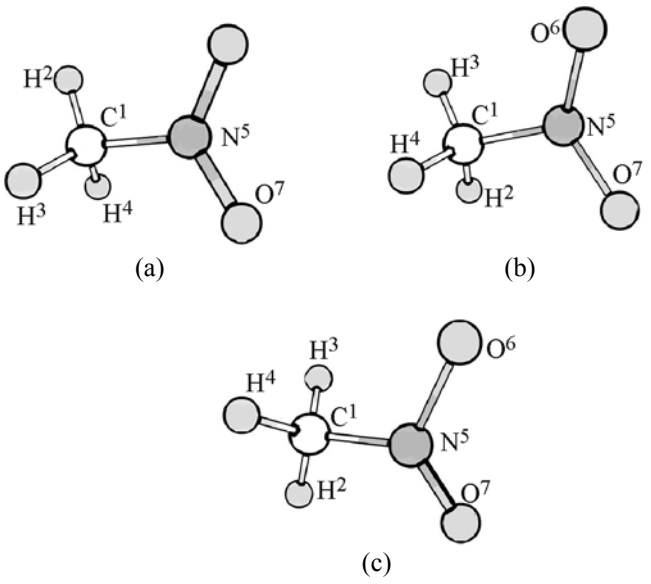

Fig. 1. Geometry structures of (a) neutral molecule, (b)cation-, and (c) anion-radicals of nitromethane.

In this work we focused our attention at the computations in the frame of the density functional theory. Primarily, that was so because high-level ab initio methods like CCSD, QCISD, and CASSCF were quite resource-consuming, making them hardly applicable to the study of the properties of real explosive (molecules of the latter usually consist of more than fifteen atoms), especially their decay mechanism.

We applied the following methods in this work: ab initio HF и MP2 [48]; non-hybrid DFT PBEPBE [49, 50], PW91PW91 [51, 52], and OLYP [53, 54]; hybrid DFT B3LYP [54, 55] and BHandHLYP [54, 56]; and double hybrid DFT B2PLYP [57] and MPW2PLYP [58]; DFT standing for the density functional theory [59, 60]. Additionally, wB97XD [61, 62] DFT method which includes empirical dispersion was employed. All the calculations were performed with 6-311+G (3df,p) basis set and GAUSSIAN 09 software [63].

Nitromethane. Nitromethane is the simplest C-nitrocompound. It is of special interest as a model to study more complex highly-energetic materials [12] as well as due to its reaction importance in various aspects of environmental issues [64]. The nitromethane molecule geometry is given in Fig. 1a. The calculated and experimental data on its geometry are collected in Table 1.

Data in Table 1 show that all the applied methods could reliably predict the bong lengths and angles in nitromethane molecule. The calculated dipole moment was also in good agreement with the experimental data (Table 2). The best results were obtained by using the non-hybrid DFT methods, PW91PW91 and PBEPBE. In general, hybrid DFT, double hybrid DFT, and ab initio MP2 and HF methods slightly overestimated the nitromethane dipole moment. The agreement with experimental values was the worst in the case of MP2 method. According to [30], dipole moments determined with the coupled clusters method including triple excitations, CCSD(T) with 6-311++G(2d,2p)

Table 1. Calculated and experimental bond lengths (Å) and bond angles (deg) in nitromethane

Method	C^1–H^2	C^1–N^5	N^5–O^6	N^5–O^7	$C^1N^5O^6$	$C^1N^5O^7$	$O^6N^5O^7$	$H^2C^1N^5$	$O^6N^5C^1H^2$
HF	1.077	1.481	1.183	1.183	117.1	117.2	125.7	108.0	153.2
MP2	1.086	1.484	1.226	1.227	116.6	117.8	125.6	108.3	180.0
PBEPBE	1.093	1.504	1.229	1.228	116.7	117.3	126.0.	108.4	161.3
PW91PW91	1.091	1.503	1.228	1.228	116.5	117.6	125.9	108.5	170.1
OLYP	1.089	1.509	1.224	1.224	116.8	117.2	126.0	108.4	158.9
B3LYP	1.085	1.499	1.218	1.218	117.0	117.3	125.7	108.2	157.6
BHandHLYP	1.078	1.481	1.198	1.198	117.1	117.2	125.9	108.1	155.0
WB97XD	1.085	1.488	1.210	1.210	116.7	117.8	125.6	108.4	177.1
MPW2PLYP	1.082	1.490	1.219	1.219	116.6	117.7	125.7	108.3	180.0
B2PLYP	1.084	1.493	1.223	1.223	116.9	117.5	125.7	108.2	161.4
Experiment [65, 66]	1.089	1.489	1.224	1.224	117.4	117.4	125.3	107.5	–

basis set, equaled 3.59 D, being the closest to the B3LYP and wB97XD methods estimations.

The relative changes of the Mulliken charges [68] in the CH_3NO_2 molecule were expressed similarly by all the employed methods, except for carbon atom. According to majority of the methods, carbon atom was slightly negatively charged; however, HF, MP2, and OLYP methods predicted small positive charge at the carbon atom (Table 3).

The analysis of nitromethane anion-radical geometry (Fig. 1, Table 4) revealed that the addition of electron to nitromethane led to slight changes of the $C^1N^5O^6$, $C^1N^5O^7$, and $O^6N^5O^7$ bond angles, whereas the bond lengths practically did not change.

Note that in contrast to the neutral molecule, the C^1–N^5–O^6–O^7 fragment in the anion-radical was not planar, which is consistent with the results of other theoretical studies carried out using different high-level ab initio methods [30, 31].

The vertical electron affinities (EA_{vert}) (Table 5), as calculated according to Eq. (1), were in all cases positive.

$$EA_v = E_{tot}(M^{\cdot-}) - E_{tot}(M_{eq}). \quad (1)$$

Here, $E_{tot}(M_{eq})$ was the total electronic energy of the molecule in the equilibrium state, $E_{tot}(M^{\cdot-})$ was the total electronic energy of the anion-radical with the geometry corresponding to the equilibrium configuretion of the molecule M_{eq}.

The estimations of adiabatic electron affinity EA_{ad} according to Eq. (2), in contrast to those obtained with HF and MP2 methods, were negative, and coincided with the experimental value [29] (Table 5).

$$EA_{ad} = E_{tot}(M_{eq}^{\cdot-}) + ZPE(M_{eq}^{\cdot-}) - E_{tot}(M_{eq}) - ZPE(M_{eq}). \quad (2)$$

Here $E_{tot}(M_{eq}^{\cdot-})$ and $E_{tot}(M_{eq})$ were the values of total electronic energy of the anion-radical and neutral molecule in their equilibrium states, respectively; ZPE $(M_{eq}^{\cdot-})$ and ZPE(M_{eq}) were zero vibrations energy of the anion-radical and the neutral molecule, respectively, as determined in the frame of DFT methods.

The best result was achieved with WB97XD method. In general, the non-hybrid and hybrid DFT methods overestimated the EA_{ad} value with respect to the experiment, whereas the double hybrid methods led to the underestimation. The ab initio methods results were not in accordance with the experiment and the DFT methods estimations. Note that the results of DFT methods were closer to the experimental EA_{ad} value than those of the high-level ab initio methods [30].

Table 2. Calculated and experimental dipole moments (D) of nitromethane, dimethylnitramine, and ethyl nitrate

Method	Nitromethane	Dimethylnitramine	Ethyl nitrate
HF	3.95	4.78	4.10
MP2	4.12	4.77	3.87
PBEPBE	3.43	4.54	3.26
PW91PW91	3.45	4.58	3.27
OLYP	3.39	4.50	3.26
B3LYP	3.61	4.74	3.57
BHandHLYP	3.74	4.79	3.83
WB97XD	3.63	4.67	3.64
MPW2PLYP	3.84	4.75	3.73
B2PLYP	3.84	4.75	3.69
Experiment	3.46 [65]	4.61 [67]	3.39 [65]

According to the computations, in the nitromethane anion-radical the absolute value of the negative charge at the oxygen atom increased and the positive charge on the nitrogen atom decreased, as compared with those in the neutral molecule (Table 6). Furthermore, the absolute value of the negative charge at the cabon atom increased and the positive charge at the hydrogen atoms decreased. It should be noted that the MP2 method was the best to predict the increase of positive charge at the carbon atom.

Similarly to the case of electron addition, its elimination (with subsequent formation of nitromethane cation-radical) had virtually no effect on the particle geometry (Table 7, Fig. 1). The geometrical parameters of nitromethane cation-radical were only slightly different from those of the neutral molecule. The ab initio MP2 method as well as double hybrid DFT methods predicted a slight elongation of the N^5–O^6 bond and shortening of the N^5–O^7 bond, whereas the data of the non-hybrid and hybrid DFT methods revealed the shortening of the N^5–O^6 and elongation of the N^5–O^7 bonds.

Note that all the applied methods pointed at decreasing of the $O^6N^5O^7$ and $H^2C^1N^5$ bond angles.

According to all employed methods, in the nitromethane cation radicals the positive charges increased

Table 3. Mulliken charges at nitromethane atoms (e. u.)

Method	C^1	H^2	H^3	H^4	N^5	O^6	O^7
HF	0.025	0.217	0.217	0.215	0.810	–0.741	–0.743
MP2	0.029	0.219	0.224	0.223	0.665	–0.670	–0.690
PBEPBE	–0.023	0.182	0.189	0.192	0.439	–0.482	–0.497
PW91PW91	–0.019	0.178	0.191	0.192	0.393	–0.455	–0.481
OLYP	0.141	0.152	0.156	0.160	0.558	–0.578	–0.588
B3LYP	–0.040	0.190	0.193	0.196	0.455	–0.493	–0.501
BHandHLYP	–0.029	0.206	0.207	0.208	0.590	–0.589	–0.594
WB97XD	–0.091	0.204	0.214	0.214	0.461	–0.486	–0.517
MPW2PLYP	–0.013	0.203	0.211	0.211	0.538	–0.564	–0.586
B2PLYP	–0.016	0.204	0.209	0.209	0.536	–0.564	–0.577

Table 4. Calculated bond lengths (Å) and bond angles (deg) in nitromethane anion-radical

Method	C^1–H^2	C^1–N^5	N^5–O^6	N^5–O^7	$C^1N^5O^6$	$C^1N^5O^7$	$O^6N^5O^7$	$H^2C^1N^5$
HF	1.074	1.488	1.188	1.188	118.0	118.0	124.0	109.2
MP2	1.092	1.459	1.300	1.300	113.4	113.4	121.6	109.0
PBEPBE	1.099	1.458	1.303	1.303	114.0	114.0	122.3	109.3
PW91PW91	1.098	1.461	1.307	1.307	113.9	113.9	122.2	109.2
OLYP	1.095	1.463	1.304	1.304	114.3	114.3	122.3	109.3
B3LYP	1.092	1.446	1.286	1.286	114.7	114.7	122.2	109.2
BHandHLYP	1.084	1.472	1.307	1.308	114.2	114.2	122.4	109.3
WB97XD	1.092	1.471	1.308	1.308	114.1	114.1	122.1	109.2
MPW2PLYP	1.089	1.478	1.303	1.302	114.2	114.3	122.0	109.1
B2PLYP	1.091	1.461	1.307	1.307	113.9	113.9	120.0	109.1

and the negative charges decreased, as compared with the neutral molecule (Table 8). The highest positive charge was localized at the nitrogen atom, whereas the negative charge was localized at the oxygen atoms. The only exceptions were the results of MP2 and HF methods. The MP2 method predicted the decrease of the charge at the carbon atom, and the HF method revealed the decrease of the charge at the nitrogen atom of the cation-radical.

The vertical ionization potentials (IP_v) were calculated according to Eq. (3).

$$IP_v = E_{tot}(M^{\cdot+}) - E_{tot}(M_{eq}). \quad (3)$$

Here $E_{tot}(HM_{eq})$ was the total electronic energy of the neutral molecule in the equilibrium state; $E_{tot}(M^{\cdot+})$ was the total electronic energy of the cation-radical with geometry corresponding to the equilibrium configuration of the neutral molecule. The calculated ionization potentials are collected in Table 9 along with the experimental values.

As seen from Table 9, all applied methods satisfactorily estimated the value of IP_v. The worst agreement with the experiment was achieved with the MP2 and BHandHLYP methods, the determined value was overestimated by 0.7 eV. The best agreement was found in the cases of non-hybrid DFT methods, PBEPBE and PW91PW91; in those cases the absolute deviation of the estimate from the experimental value was only 0.03 and 0.05 eV, respectively.

The ionization potential as estimated by using the Koopmans theorem (IP_K), the absolute energy of the highest occupied molecular orbital, were in poor agreement with the experiment in the case of non-hybrid DFT methods (Table 9). The most reliable

Table 5. Calculated and experimental electron affinities of nitromethane, dimethylnitramine, and ethyl nitrate (eV)

Method	Nitromethane		Dimethylnitramine		Ethyl nitrate	
	EA_v	EA_{ad}	EA_v	EA_{ad}	EA_v	EA_{ad}
HF	1.05	1.46	1.52	0.39	1.26	0.0
MP2	0.80	0.21	1.26	0.25	1.06	–0.21
PBEPBE	0.30	–0.23	0.47	–	0.36	–1.18
PW91PW91	0.24	–0.30	0.43	–	0.30	–1.25
OLYP	0.49	–0.03	0.66	–	1.05	–
B3LYP	0.24	–0.40	0.55	–0.25	0.42	–1.32
BHandHLYP	0.41	–0.32	0.92	–0.10	0.66	–
WB97XD	0.43	–0.25	0.93	–0.07	0.69	–0.95
MPW2PLYP	0.29	–0.19	0.75	–0.07	0.45	–0.91
B2PLYP	0.29	–0.15	0.75	–0.05	0.44	–0.92
Experiment	–	–0.26±0.08 [29]	–	–	–	–

Table 6. Mulliken charges at nitromethane anion-radical (e. u.)

Method	C^1	H^2	H^3	H^4	N^5	O^6	O^7
HF	–1.867	0.434	0.434	0.416	0.973	–0.690	–0.700
MP2	0.064	0.143	0.143	0.142	0.258	–0.875	–0.875
PBEPBE	–0.252	0.141	0.141	0.142	0.067	–0.619	–0.619
PW91PW91	–0.256	0.142	0.142	0.140	0.002	–0.585	–0.585
OLYP	–0.106	0.116	0.116	0.114	0.065	–0.652	–0.652
B3LYP	–0.128	0.129	0.123	0.129	0.083	–0.669	–0.669
BHandHLYP	–0.041	0.138	0.138	0.130	0.165	–0.765	–0.765
WB97XD	–0.118	0.148	0.138	0.135	0.121	–0.699	–0.725
MPW2PLYP	–0.030	0.138	0.138	0.134	0.129	–0.754	–0.754
B2PLYP	–0.026	0.135	0.135	0.130	0.137	–0.756	–0.756

results were obtained with the BHandHLYP, wB97XD, MPW2PLYP, and B2PLYP methods.

To conclude, all employed quantum-chemical methods gave reliable estimations of bond lengths, bond angles, and dipole moment of the neutral nitromethane molecule. The geometry parameters of the anion-radical and the cation-radical obtained from different quantum-chemical methods were in good with each other. In the adiabatic electron affinity estimation, DFT methods were the best, whereas the results of HF and MP2 were in poorer agreement with the experiment. In contrast to EA_{ad} values, the computed vertical ionization potential agree well with the experimental value.

Dimethylnitramine. The interest to dimethylnitramine [69–74] is due to the possibility of its application as a model of efficient explosives: 1,3,5,7-tetranitro-1,3,5,7-tetraazacyclooctane (octogen) and 1,3,5-trinitro-1,3,5-triazacyclohexane (hexogen).

Similarly to the case of nitromethane, the computational methods predict geometry (Fig. 2, Table 10) and dipole moment (Table 2) of the neutral dimethylnitramine molecule quite reliably.

Note that all applied methods significantly underestimated the value of the $C^6N^1C^2$ angle as compare to experiment.

The computational estimations of dimethylnitramine dipole moment in this work were in better

Table 7. Calculated bond lengths (Å) and bond angles (deg) in nitromethane cation-radical

Method	C^1–H^2	C^1–N^5	N^5–O^6	N^5–O^7	$C^1N^5O^6$	$C^1N^5O^7$	$O^6N^5O^7$	$H^2C^1N^5$
HF	1.081	1.498	1.233	1.240	122.1	120.6	117.2	106.1
MP2	1.089	1.488	1.345	1.105	110.6	128.1	121.3	105.5
PBEPBE	1.103	1.457	1.239	1.239	124.2	127.4	111.5	107.5
PW91PW91	1.100	1.456	1.238	1.238	124.4	126.4	111.5	107.4
OLYP	1.098	1.464	1.235	1.235	124.2	124.7	111.3	107.4
B3LYP	1.093	1.467	1.226	1.225	124.6	113.7	110.7	107.1
BHandHLYP	1.086	1.485	1.149	1.297	126.9	124.3	119.5	105.9
WB97XD	1.092	1.475	1.166	1.293	127.5	124.1	118.0	108.2
MPW2PLYP	1.091	1.488	1.307	1.167	113.0	124.4	119.6	105.4
B2PLYP	1.090	1.476	1.365	1.163	115.6	114.4	118.0	107.8

Table 8. Mulliken charges at nitromethane cation-radical atoms (e. u.)

Method	C^1	H^2	H^3	H^4	N^5	O^6	O^7
HF	0.042	0.278	0.269	0.281	0.655	–0.281	–0.245
MP2	–0.002	0.280	0.284	0.284	0.864	–0.192	–0.518
PBEPBE	0.042	0.255	0.255	0.269	0.569	–0.196	–0.195
PW91PW91	0.052	0.248	0.257	0.268	0.558	–0.185	–0.199
OLYP	0.202	0.225	0.221	0.238	0.688	–0.289	–0.284
B3LYP	–0.003	0.261	0.258	0.273	0.575	–0.183	–0.179
BHandHLYP	–0.023	0.280	0.272	0.272	0.675	–0.377	–0.099
WB97XD	–0.053	0.259	0.284	0.284	0.613	–0.287	–0.100
MPW2PLYP	–0.006	0.282	0.256	0.282	0.657	–0.129	–0.342
B2PLYP	0.015	0.262	0.275	0.275	0.538	–0.118	–0.248

agreement with the experiment than those presented in [75].

The analysis of the atomic charges (Table 11) revealed that the negative charge was mainly localized at the amino group nitrogen and at the nitro group oxygen atoms. A slight negative charged was found at the carbon atoms. The positive charge was localized at the hydrogen atoms and the nitro group nitrogen.

Prior to discussion of the results obtained during computation of dimethylnitramine anion-radical, it should be noted that the geometry parameters calculated using non-hybrid DFT methods (PBEPBE, OLYP, and PW91PW91) were in poor agreement with the results of other methods, and are thus doubtful. For example, according to the PBEPBE and PW91PW91 methods, the N–N bond length in the anion-radical was 4.774 and 4.680 Å, respectively. Moreover, the $N^{10}N^1C^2H^4$ torsion angle (its change corresponding to the rotation around the N^1–C^2 bond in the anion-radical) equaled –102.5° according to the PBEPBE and PW91PW91 methods, being –52.2° in the neutral molecule. The attempts to localize the dimethylnitramine anion-radical structure corresponding to the minimum at the potential energy surface by means of the OLYP method failed. In the course of geometry optimization the length of N–N bond reached 10.6 Å, and then the procedure was terminated reaching the

Table 9. Calculated and experimental ionization potentials of neutral molecules of nitromethane, dimethylnitramine, and ethyl nitrate (eV)

Method	Nitromethane		Dimethylnitramine		Ethyl nitrate	
	IP_v	IP_K	IP_v	IP_K	IP_v	IP_K
HF	11.32	12.63	9.22	11.44	11.41	13.05
MP2	11.74	12.50	10.33	11.55	11.92	13.07
PBEPBE	11.05	6.97	10.18	6.52	10.84	7.46
PW91PW91	11.13	7.05	10.25	6.60	10.92	7.54
OLYP	10.93	6.86	9.55	6.38	10.72	7.31
B3LYP	11.50	8.53	9.99	7.73	11.50	8.91
BHandHLYP	11.77	10.60	10.04	9.28	11.89	10.89
WB97XD	11.60	10.75	10.05	9.81	11.74	11.06
MPW2PLYP	11.59	10.63	9.86	9.42	11.65	11.00
B2PLYP	11.53	10.47	9.81	9.27	11.59	10.85
Experiment [65]	11.08		9.53		11.22	

Table 10. Calculated and experimental values of bond lengths (Å) and bond angles (deg) in dimethylnitramine

Method	N^1–N^{10}	N^1–C^2	N^{10}–O^{11}	C^2–H^3	$H^3C^2N^1$	$C^6N^1C^2$	$C^2N^1N^{10}$	$N^1N^{10}O^{11}$	$O^{11}N^{10}O^{12}$
HF	1.345	1.453	1.189	1.080	107.0	119.5	115.7	117.4	125.1
MP2	1.379	1.453	1.227	1.090	107.0	118.1	114.0	117.0	126.0
PBEPBE	1.395	1.454	1.233	1.098	107.5	119.8	115.7	116.8	126.0
PW91PW91	1.393	1.454	1.233	1.096	107.5	120.0	115.8	116.8	126.2
OLYP	1.397	1.456	1.229	1.093	107.5	119.6	116.0	116.9	126.1
B3LYP	1.376	1.455	1.224	1.089	107.4	120.4	116.0	117.1	125.8
BHandHLYP	1.350	1.446	1.205	1.079	110.1	120.6	116.0	117.2	125.5
WB97XD	1.368	1.44941	1.215	1.087	110.0	119.9	115.7	117.2	125.6
MPW2PLYP	1.375	1.45299	1.223	1.084	110.0	119.4	115.1	117.1	125.8
B2PLYP	1.381	1.45541	1.227	1.085	109.9	119.3	115.0	117.1	125.9
Experiment [66]	1.382	1.460	1.223	1.121	101.9	127.6	116.2	114.8	130.4

maximum number of the optimization cycles. Thus, we decided to omit the data on dimethylnitramine geometry and atomic charges obtained by means of the non-hybrid DFT methods.

In general, the geometry parameters of dimethylnitramine anion-radical (Fig. 3) obtained in this work are in good agreement (Table 12). The exceptions were the above-mentioned non-hybrid DFT methods, their application to the anion-radical studies was not rational.

According to the quantum-chemical methods, the addition of electron to dimethylnitramine led to elongation of the N^1–N^{10} bond (by 0.143 Å on the average) and to decrease of the $C^2N^1C^6$, $C^2N^1N^{10}$, and

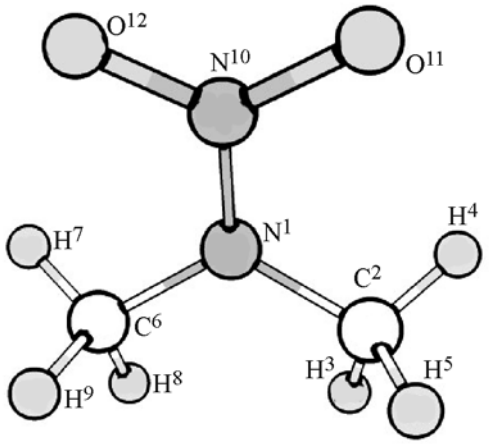

Fig. 2. Geometry structure of dimethylnitramine.

$O^{11}N^{10}O^{12}$ bond angles (on the average, by 8.4°, 6.6°, and 3.5°, respectively). The N–N bond elongation in the anion-radical as compared with the neutral molecule was accompanied with the $N^{10}N^{1}C^{2}C^{4}$ torsion angle change from –55.0° to 175°.

The analysis of the atomic charges (Table 13) revealed that the electron addition led to significant increase of the absolute value of the negative charge at the N^{1}, O^{11}, and O^{12}.

Similarly to the case of nitromethane, the vertical ionization potential EA_v of dimethylnitramine as calculated according to Eq. (1) was positive (Table 5). According to the ab initio methods, HF and MP2, the adiabatic electron affinity was positive. In contrast to the ab initio methods estimations, the adiabatic electron affinity derived from the DFT methods was negative. Similar trend was noticed in the case of nitromethane as well.

In general, the calculated EA_{ad} values for dimethylnitramine were significantly lower than those in the case of nitromethane. Unfortunately, the experimental values of the vertical and adiabatic electron affinity of dimethylnitramine could not be found in the literature. Experimental value of dimethylnitramine ionization potential was by 1.55 eV lower than that of nitromethane (Table 9).

The best estimation of calculated vertical ionization potential of dimethylnitramine was only 0.02 eV over the experimental value of IP_v. Two other non-hybrid DFT methods, PBEPBE and PW91PW91, that reliably estimated the ionization potential of nitromethane, worked worse than the other DFT methods in the case of dimethylnitramine. In general, the MP2 method estimate was in the worst agreement with the experiment, overestimating the IP_v value by 0.8 eV. The mean absolute deviation from the experiment was 0.46 eV in the case of hybrid and double hybrid methods. The double hybrid methods, MPW2PLYP and B2PLYP, overestimated IP_v by 0.33 and 0.28 eV, respectively. Those two methods also quite accurately expressed the ionization potential IP_K as calculated according the Koopmans theorem. From Table 13, the absolute deviation was of 0.11 eV in the case of

Table 11. Mulliken charges at dimethylnitramine atoms (e. u.)

Method	N^1	C^2	H^3	H^4	H^5	C^6	H^7	H^8	H^9	N^{10}	O^{11}	O^{12}
HF	–0.428	–0.065	0.176	0.197	0.192	–0.065	0.197	0.176	0.192	0.899	–0.735	–0.735
MP2	–0.483	–0.067	0.180	0.200	0.196	–0.067	0.200	0.180	0.196	0.796	–0.665	–0.665
PBEPBE	–0.335	–0.117	0.156	0.180	0.165	–0.119	0.180	0.157	0.164	0.554	–0.492	–0.493
PW91PW91	–0.317	–0.123	0.155	0.179	0.164	–0.125	0.179	0.155	0.164	0.506	–0.468	–0.469
OLYP	–0.443	0.052	0.127	0.145	0.131	0.051	0.146	0.128	0.131	0.722	–0.595	–0.596
B3LYP	–0.307	–0.129	0.157	0.182	0.169	–0.129	0.182	0.157	0.169	0.538	–0.496	–0.496
BHandHLYP	–0.341	–0.125	0.194	0.169	0.184	–0.125	0.169	0.194	0.183	0.675	–0.589	–0.589
wB97XD	–0.291	–0.191	0.200	0.174	0.190	–0.188	0.173	0.199	0.190	0.542	–0.498	–0.499
mPW2PLYP	–0.381	–0.110	0.194	0.170	0.184	–0.110	0.170	0.194	0.184	0.644	–0.569	–0.569
B2PLYP	–0.380	–0.110	0.193	0.169	0.182	–0.110	0.169	0.193	0.182	0.636	–0.562	–0.562

Table 12. Calculated and experimental values of bond lengths (Å) and bond angles (deg) in dimethylnitramine anion-radical

Method	N^1–N^{10}	N^1–C^6	N^{10}–O^{11}	N^{10}–O^{12}	C^2–H^3	$H^3C^2N^1$	$C^6N^1C^2$	$C^2N^1N^{10}$	$N^1N^{10}O^{11}$	$O^{11}N^{10}O^{12}$
HF	1.432	1.443	1.268	1.268	1.077	109.8	111.7	110.6	113.6	122.5
MP2	1.542	1.449	1.278	1.278	1.089	109.0	110.0	107.0	111.1	122.1
B3LYP	1.559	1.447	1.283	1.283	1.088	108.8	111.8	108.6	111.5	122.2
BHandHLYP	1.465	1.439	1.274	1.274	1.079	109.2	111.7	109.9	112.7	122.3
wB97XD	1.500	1.444	1.280	1.280	1.088	109.1	111.2	109.1	112.1	122.1
mPW2PLYP	1.524	1.447	1.284	1.284	1.086	109.0	111.1	108.4	111.7	122.1
B2PLYP	1.551	1.448	1.285	1.285	1.087	108.9	111.1	108.0	111.3	122.1

Table 13. Mulliken charges at dimethylnitramine anion-radical atoms (e. u.)

Method	N^1	C^2	H^3	H^4	H^5	C^6	H^7	H^8	H^9	N^{10}	O^{11}	O^{12}
HF	–0.605	–0.059	0.187	0.125	0.135	–0.059	0.125	0.187	0.135	0.654	–0.912	–0.912
MP2	–0.671	–0.069	0.192	0.122	0.138	–0.069	0.122	0.192	0.138	0.648	–0.871	–0.871
B3LYP	–0.374	–0.182	0.166	0.105	0.101	–0.182	0.105	0.166	0.101	0.236	–0.621	–0.621
BHandHLYP	–0.439	–0.149	0.182	0.119	0.120	–0.150	0.119	0.182	0.120	0.393	–0.748	–0.748
wB97XD	–0.429	–0.213	0.187	0.125	0.128	–0.213	0.124	0.187	0.128	0.317	–0.670	–0.670
mPW2PLYP	–0.490	–0.142	0.182	0.117	0.123	–0.142	0.117	0.182	0.123	0.397	–0.734	–0.734
B2PLYP	–0.513	–0.131	0.179	0.114	0.119	–0.131	0.114	0.179	0.119	0.406	–0.728	–0.728

MPW2PLYP and 0.26 eV in the case of B2PLYP. The calculated estimates of IP_K obtained by means of wB97XD and BHandHLYP method were also in satisfactory agreement with the experiment. The hybrid B3LYP and the non-hybrid PBEPBE, PW91PW91, and OLYP methods significantly underestimated the IP_K value, whereas HF and MP2 methods led to its overestimation. Note that the same trend was observed in the case of nitromethane.

In contrast to the case of dimethylnitramine anion-radical, the geometry of its cation-radical as obtained from the hybrid OLYP, PBEPBE, and PW91PW91 DFT methods were in good agreement with the results of other methods. The cation-radical geometry is shown in Fig. 4, the geometry parameters are collected in Table 14.

The bond lengths and bond angles calculated by different quantum-chemical methods were in good agreement. As compared with the neutral molecule, in dimethylnitramine cation radical the N^1–N^{10} bond was elongated by 0.270 Å. The highest estimate of that bond elongation (0.389 Å) was obtained in the OLYP method. All applied methods predicted the decrease of

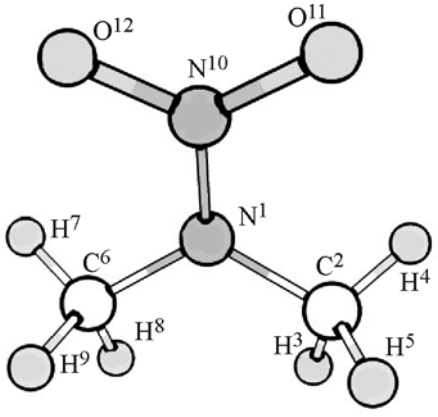

Fig. 3. Geometry structure of dimethylnitramine anion-radical.

Table 14. Calculated and experimental values of bond lengths (Å) and bond angles (deg) in dimethylnitramine cation-radical

Method	N^1–N^{10}	N^1–C^6	N^{10}–O^{11}	C^2–H^3	$H^3C^2N^1$	$C^6N^1C^2$	$C^2N^1N^{10}$	$N^1N^{10}O^{11}$	$O^{11}N^{10}O^{12}$
HF	1.467	1.462	1.160	1.080	109.1	125.2	115.7	117.4	132.9
MP2	1.580	1.419	1.190	1.098	109.0	125.8	115.8	113.1	135.3
PBEPBE	1.755	1.412	1.183	1.099	110.4	127.4	116.3	111.0	138.1
PW91PW91	1.753	1.412	1.182	1.097	110.3	127.5	116.2	111.0	138.0
OLYP	1.786	1.417	1.177	1.094	110.8	126.3	116.9	110.7	138.5
B3LYP	1.685	1.421	1.175	1.089	110.4	126.2	116.9	111.6	136.8
BHandHLYP	1.533	1.426	1.168	1.089	109.0	125.2	116.0	113.5	133.9
wB97XD	1.578	1.419	1.176	1.096	109.6	125.8	115.9	113.1	134.8
mPW2PLYP	1.643	1.423	1.179	1.087	110.2	125.8	117.3	111.8	136.3
B2PLYP	1.680	1.422	1.181	1.089	110.2	126.0	117.0	111.5	137.0

Table 15. Mulliken charges at dimethylnitramine cation-radical atoms (e. u.)

Method	N^1	C^2	H^3	H^4	H^5	C^6	H^7	H^8	H^9	N^{10}	O^{11}	O^{12}
HF	–0.280	–0.107	0.265	0.239	0.272	–0.107	0.239	0.272	0.265	1.082	–0.571	–0.571
MP2	–0.416	–0.080	0.271	0.244	0.271	–0.146	0.273	0.269	0.273	1.000	–0.491	–0.469
PBEPBE	–0.422	–0.100	0.228	0.245	0.244	–0.100	0.244	0.228	0.245	0.775	–0.293	–0.293
PW91PW91	–0.418	–0.097	0.226	0.243	0.243	–0.097	0.243	0.227	0.243	0.772	–0.293	–0.293
OLYP	–0.583	0.058	0.198	0.210	0.216	0.057	0.216	0.198	0.210	1.014	–0.397	–0.397
B3LYP	–0.349	–0.129	0.237	0.241	0.251	–0.130	0.251	0.237	0.242	0.750	–0.300	–0.300
BHandHLYP	–0.143	–0.119	0.265	0.236	0.278	–0.119	0.236	0.265	0.278	0.705	–0.441	–0.441
wB97XD	–0.275	–0.161	0.268	0.234	0.272	–0.214	0.271	0.256	0.269	0.746	–0.342	–0.322
mPW2PLYP	–0.383	–0.133	0.252	0.261	0.254	–0.126	0.250	0.253	0.261	0.861	–0.373	–0.376
B2PLYP	–0.390	–0.134	0.250	0.252	0.260	–0.134	0.260	0.250	0.252	0.847	–0.356	–0.356

the $N^1N^{10}O^{11}$ bond angle (by 4.6° on the average) and the increase in the $C^2N^1N^{10}$ and $O^{11}N^{10}O^{12}$ bond angles (on the average, by 6.5 and 10.4°, respectively).

The atomic charges data is shown in Table 15. Note that the atomic charge values in dimethylnitramine cation-radical as derived by different methods were quite controversial.

In contrast to anion-radical (in that case all applied methods predicted the increase in the absolute negative charge and decrease in the positive charge with respect to the neutral molecule), in the case of the cation-radical the common trend was not revealed. Probably, the most reliable data were obtained by means of the BHandHLYP method. In particular, in dimethylnitramine cation-radical, the negative charges at N^1 and at the oxygen atoms were significantly decreased, whereas the absolute negative charge at the carbon atoms was slightly decreased and the positive charge at the hydrogen atoms was increased.

All applied DT-based methods, except for BHandHLYP and wB97XD, predicted the increase in the absolute value of the negative charge at N^1 upon cation-radical formation from the neutral molecule.

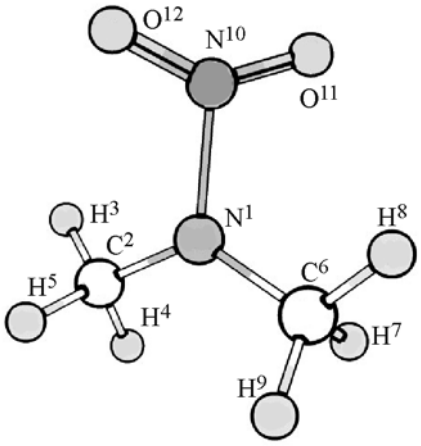

Fig. 4. Geometry structure of dimethylnitramine cation-radical.

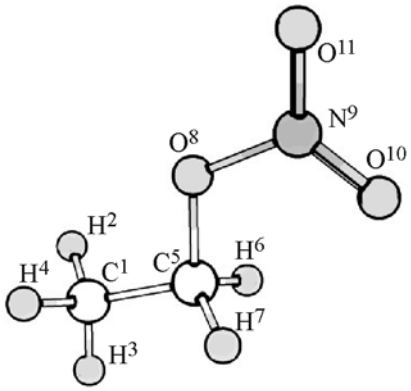

Fig. 5. Geometry structure of ethyl nitrate.

Note that according to B3LYP, wB97XD, B2PLYP, and mPW2PLYP methods, the absolute negative charge at C^6 was higher in dimethylnitramine cation-radical than that in the neutral molecule, being consistent with results of the double hybrid B2PLYP and mPW2PLYP methods. The atomic charges data obtained from the ab initio HF and MP2 methods revealed that elimination of electron from dimethylnitramine neutral molecule led to the decrease in the absolute value of the N^1 negative charge, that observation being in agreement with the BHandHLYP and wB97XD methods. Furthermore, the HF and MP2 method revealed the decrease in the absolute values of the C^2 and C^6 negative charges upon formation of the cation-radical, that result being confirmed by the double hybrid DFT methods.

To conclude, all applied quantum-chemical methods could predict well dimethylnitramine neutral molecule and its cation-radical geometries; however, in the case of the corresponding anion-radical, the use of PBEPBE, PW91PW91, and OLYP methods did not lead to reliable results. The trends observed for calculations of the ionization potential and the electron affinity were similar to those in the case of nitromethane. All applied methods satisfactory estimated the vertical ionization potential calculated on the basis of electron energy without accounting for the zero

Table 16. Calculated and experimental values of bond lengths (Å) and bond angles (deg) in ethyl nitrate

Method	C^1–C^5	C^5–O^8	O^8–N^9	N^9–O^{10}	N^9–O^{11}	$C^1C^5O^8$	$C^5O^8N^9$	$O^8N^9O^{10}$	$O^8N^9O^{11}$	$O^{10}N^9O^{11}$
HF	1.510	1.434	1.324	1.179	1.170	105.8	116.6	116.0	118.0	127.9
MP2	1.515	1.447	1.449	1.213	1.204	105.9	113.2	117.0	112.4	129.9
PBEPBE	1.516	1.448	1.449	1.213	1.205	105.9	113.3	117.0	112.3	130.6
PW91PW91	1.515	1.447	1.449	1.213	1.204	105.9	113.2	117.0	112.4	130.6
OLYP	1.519	1.446	1.445	1.209	1.202	106.3	114.3	117.4	112.1	130.4
B3LYP	1.514	1.449	1.408	1.206	1.197	105.9	114.5	117.4	112.9	129.6
BHandHLYP	1.504	1.435	1.356	1.191	1.182	105.8	115.3	117.7	113.6	128.71
WB97XD	1.510	1.438	1.381	1.200	1.192	105.9	114.6	117.6	113.2	129.2
MPW2PLYP	1.510	1.444	1.397	1.206	1.198	105.5	114.1	117.4	113.0	129.5
B2PLYP	1.511	1.446	1.408	1.210	1.202	105.5	113.9	117.4	112.9	129.7
Experiment [65]	1.528	1.430	1.407	1.215	1.215	109.47	111.0	118.0	111.0	–

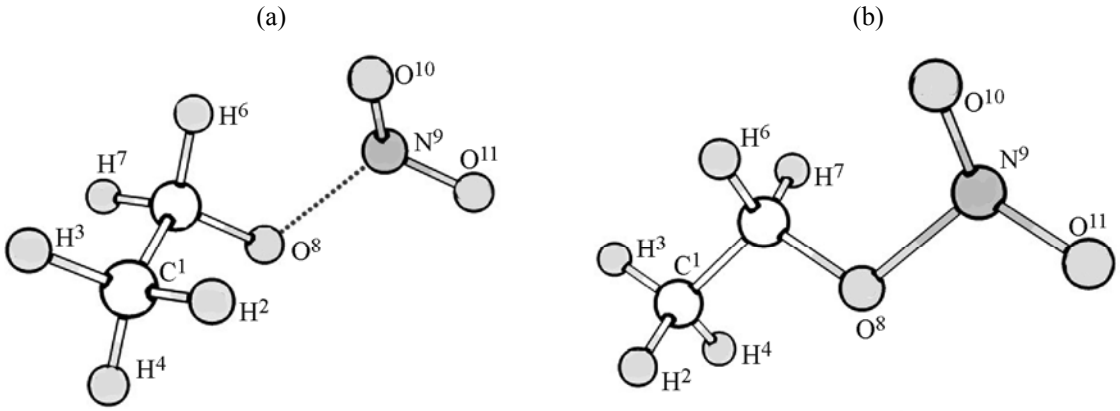

Fig. 6. Equilibrium geometry structures of ethyl nitrate anion-radical according to (a) B3LYP, PBEPBE, PW91PW91, wB97XD, MPW2PLYP, B2PLYP and (b) HF, MP2 methods.

vibrations. The double hybrid methods were the best to estimate the ionization potential as calculated according to the Koopmans theorem.

Ethyl nitrate. Ethyl nitrate is a model compound for studies of pentaerythritol tetranitrate, an explosive widely used in mining. Also, this compound is used in medicine for stenocardia and ischemic syndrome prevention; with nitroglycerine, it belongs to the group of vasodilators.

The geometry of ethyl nitrate is shown in Fig. 5.

The analysis of calculated geometry parameters (Table 16) revealed good agreement between calculated and experimental data. Similarly to nitromethane and dimethylnitramine, the computed dipole moments were agreement with the experiment (Table 2).

The analysis of the atomic charges (Table 17) revealed that the negative charge was localized at C^1 and the oxygen atoms. The highest positive charge was localized at the nitrogen atom.

In the equilibrium structure of ethyl nitrate anion-radical (Fig. 6), according to the DFT methods, the O^8–N^9 was significantly elongated as compared with the neutral molecule (on the average, by 0.805 Å) (Tables 16 and 18).

Table 17. Mulliken charges at ethyl nitrate atoms (e. u.)

Method	C^1	H^2	H^3	H^4	C^5	H^6	H^7	O^8	N^9	O^{10}	O^{11}
HF	–0.598	0.197	0.189	0.197	0.218	0.185	0.185	–0.672	1.535	–0.709	–0.726
MP2	–0.604	0.198	0.188	0.198	0.232	0.184	0.184	–0.645	1.292	–0.606	–0.621
PBEPBE	–0.575	0.174	0.170	0.174	0.179	0.158	0.158	–0.453	0.884	–0.418	–0.450
PW91PW91	–0.574	0.174	0.169	0.174	0.172	0.159	0.159	–0.435	0.842	–0.402	–0.438
OLYP	–0.496	0.140	0.137	0.139	0.343	0.113	0.113	–0.519	1.106	–0.514	–0.563
B3LYP	–0.562	0.176	0.173	0.176	0.168	0.168	0.168	–0.471	0.910	–0.443	–0.462
BHandHLYP	–0.584	0.189	0.184	0.189	0.163	0.182	0.182	–0.536	1.150	–0.550	–0.571
WB97XD	–0.582	0.188	0.182	0.188	0.181	0.180	0.180	–0.544	1.078	–0.516	–0.535
MPW2PLYP	–0.610	0.196	0.189	0.196	0.102	0.186	0.186	–0.469	0.945	–0.454	–0.466
B2PLYP	–0.583	0.187	0.181	0.187	0.186	0.178	0.178	–0.543	1.056	–0.505	–0.522

Table 18. Calculated values of bond lengths (Å) and bond angles (deg) in ethyl nitrate anion-radical

Method	C^1–C^5	C^5–O^8	O^8–N^9	N^9–O^{10}	N^9–O^{11}	$C^1C^5O^8$	$C^5O^8N^9$	$O^8N^9O^{10}$	$O^8N^9O^{11}$	$O^{10}N^9O^{11}$
HF	1.518	1.387	1.420	1.260	1.245	107.7	112.4	113.1	110.1	124.1
MP2	1.521	1.391	1.606	1.254	1.245	108.2	109.8	110.8	106.7	125.6
PBEPBE	1.546	1.360	2.329	1.239	1.233	114.0	102.8	111.0	115.1	123.5
PW91PW91	1.545	1.360	2.298	1.239	1.232	113.9	103.1	111.0	114.3	123.6
B3LYP	1.539	1.362	2.327	1.229	1.224	114.2	100.9	113.0	117.0	122.7
WB97XD	1.533	1.360	2.241	1.223	1.216	113.8	100.9	114.5	116.4	122.6
MPW2PLYP	1.536	1.361	2.059	1.222	1.215	112.8	107.6	111.9	109.5	125.4
B2PLYP	1.539	1.362	2.066	1.225	1.219	112.8	108.1	111.6	109.1	125.7

Similarly to dimethylnitramine anion-radical, the equilibrium configuration could not be found for ethyl nitrate anion-radical by means of the OLYP method. However, in the case of ethyl nitrate anion-radical, the data obtained from the non-hybrid DFT methods PBEPBE and PW91PW91 were consostent with other estimates of DFT methods. According to BHandHLYP, the O^8–N^9 bond length was of 4.472 Å. From the ab initio MP2 and HF methods, this bond in the anion-radical (Fig. 6b, Table 18) was only by 0.096 Å and 0.157 Å, respectively, longer than that in the neutral molecule. The PBEPBE, PW91PW91, B3LYP, and wB97XD methods predicted the decrease in the $C^5O^8N^9$ bond angle upon formation of the anion radical (by 10.5°, 10.1°, 13.6°, and 13.7°, respectively), whereas the corresponding decrease as determined from the ab initio and double empirical DFT methods did not exceed 6.5°. All applied methods predicted the decrease of the $O^{10}N^9O^{11}$ angle (on the average, by 5.4°).

The analysis of Mulliken atomic charges in the anion-radical of ethyl nitrate (Table 19) revealed the following changes with respect to the neutral molecule: decrease in the positive charge at the hydrogen atoms, decrease in the absolute value of the C^1 negative charge, decrease in the absolute value of the O^8 negative charge, and a significant decrease in the positive charge at N^9.

All DFT methods, except for MPW2PLYP and B2PLYP, predicted the negative charge at C^5. In contrast to the DFT methods, the ab initio HF and MP2 methods predicted the increase of positive charge at C^5 with respect to the neutral molecule. Interestingly, the

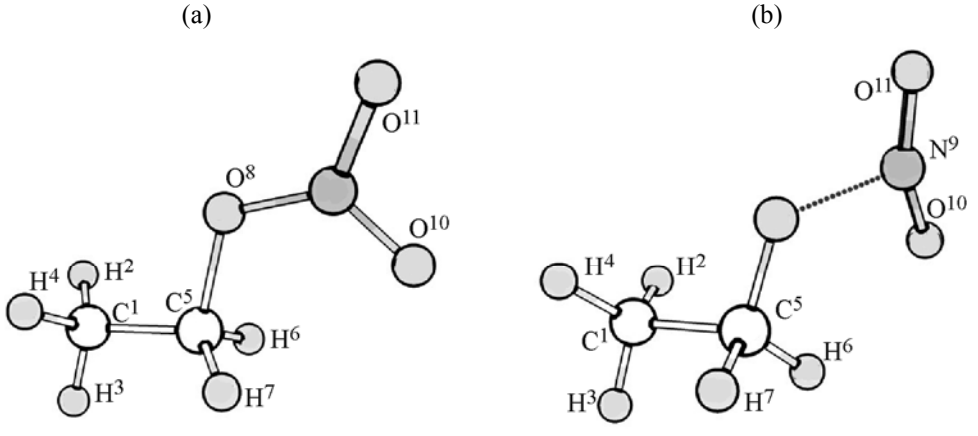

Fig. 7. Equilibrium geometry of ethyl nitrate cation-radical according to (a) HF, MP2, BHandHLYP, wB97XD, MPW2PLYP, B2PLYP and (b) B3LYP, PBEPBE, PW91PW91, OLYP methods.

Table 19. Mulliken charges at ethyl nitrate anion-radical atoms (e. u.)

Method	C^1	H^2	H^3	H^4	C^5	H^6	H^7	O^8	N^9	O^{10}	O^{11}
HF	–0.559	0.163	0.140	0.163	0.244	0.153	0.119	–0.672	0.958	–0.876	–0.834
MP2	–0.566	0.161	0.133	0.157	0.256	0.151	0.102	–0.748	0.886	–0.793	–0.740
PBEPBE	–0.467	0.160	0.110	0.134	–0.024	0.152	0.069	–0.597	0.157	–0.336	–0.359
PW91PW91	–0.476	0.166	0.115	0.139	–0.069	0.162	0.077	–0.570	0.070	–0.292	–0.322
B3LYP	–0.443	0.128	0.110	0.154	0.008	0.079	0.158	–0.622	0.229	–0.424	–0.378
WB97XD	–0.502	0.186	0.127	0.144	–0.012	0.159	0.085	–0.600	0.239	–0.408	–0.419
MPW2PLYP	–0.509	0.139	0.121	0.164	0.106	0.078	0.164	–0.647	0.370	–0.487	–0.498
B2PLYP	–0.512	0.141	0.123	0.169	0.093	0.083	0.170	–0.639	0.349	–0.480	–0.497

B3LYP, PBEPBE, PW91PW91, wB97XD, and B2PLYP methods predicted the decrease in the absolute value of negative charge at O^{10} and O^{11} upon the anion-radical formation, oppo-sitely to the ab initio HF and MP2 methods. That could be explained by the longer O^8–N^9 bond in the anion-radical as estimated by the DFT methods.

Similarly to the case of nitromethane and dimethylnitramine, the vertical affinity values EA_{vert} (Table 5) as calculated according to Eq. (1) were positive. The adiabatic electron affinity in the frame of the HF method was zero. Interestingly, the EA_{ad} value as calculated by means of MP2 methods was negative, whereas in the cases of nitromethane and dimethyl-nitramine the same method gave positive estimates of EA_{ad}. However, it should be noted that the MP2 method significantly overestimated EA_{ad} as compared with other methods.

Equilibrium structures of ethyl nitrate cation-radical and their geometry parameters are given in Fig. 7 and Table 20. From the presented data, the calculated geometry parameters significantly depended on the applied quantum-chemical method.

According to the HF and MP2 methods, as well as to BHandHLYP, wB97XD, MPW2PLYP, and B2PLYP DFT methods, the bond elongation upon formation of the cation-radical was only of 0.1 Å.

The O^8–N^9 bond length as computed with the non-hybrid PBEPBE, PW91PW91, and OLYP methods and with the hybrid B3LYP method was significantly longer than 1.9 Å. Besides O^8–N^9 elongation, the formation of the cation-radical was accompanied by rotation of the nitro group with respect to the O–NO_2 bond. In particular, according to the B3LYP, PBEPBE, PW91PW91, and OLYP methods, the $C^1C^5O^8N^9$ dihedral angle was of –110.7, 140.5, 133.3, and –140.7°, respectively. According to the named methods, in the cation-radical the $O^{10}N^9O^{11}$ bond angle increased by 19.3° on the average with respect to the neutral molecule.

The ab initio HF and MP2 methods, the double hybrid DFT methods, as well as BHandHLYP and wB97XD methods predicted the decrease of the $O^{10}N^9O^{11}$ angle by 12.4° on the average and the shortening of the O^8–N^9 bond by 0.125 Å on the average upon formation of the cation-radical.

Inspection of atomic charges (Table 21) revealed the following changes upon formation of the cation radical: the decrease in the absolute value of the negative charges at oxygen atoms and C^1, significant increase in the positive charge at the nitrogen atom, and slight increase in the positive charges at the hydrogen atoms.

The estimations of charges by means of the wB97XD method was in disagreement with the other levels of theory: according to wB97XD, the absolute value of the negative charge at C^1 and the positive charge at the nitrogen atom were slightly increased. Furthermore, all the methods but MPW2PLYP predicted the decrease of the positive charge at C^5 in the cation-radical as compared with the neutral molecule.

The experimental ionization potential of ethyl nitrate (Table 9) was practically the same as that of nitromethane (11.08 eV).

Table 20. Calculated values of bond lengths (Å) and bond angles (deg) in ethyl nitrate cation-radical

Method	C^1–C^5	C^5–O^8	O^8–N^9	N^9–O^{10}	N^9–O^{11}	$C^1C^5O^8$	$C^5O^8N^9$	$O^8N^9O^{10}$	$O^8N^9O^{11}$	$O^{10}N^9O^{11}$
HF	1.497	1.588	1.220	1.203	1.186	104.0	119.3	125.9	123.4	110.7
MP2	1.496	1.537	1.276	1.237	1.222	104.1	114.4	125.3	122.6	112.2
PBEPBE	1.560	1.335	1.971	1.164	1.157	113.6	114.7	107.9	103.4	148.7
PW91PW91	1.577	1.333	1.965	1.163	1.157	112.4	114.6	107.9	103.5	148.6
OLYP	1.561	1.336	2.047	1.158	1.153	113.7	118.0	108.0	101.9	150.1
B3LYP	1.613	1.333	1.981	1.146	1.140	107.8	116.4	106.8	102.1	151.1
BHandHLYP	1.489	1.550	1.254	1.152	1.308	104.8	116.4	129.4	111.1	119.5
WB97XD	1.493	1.558	1.263	1.175	1.286	104.9	116.0	129.1	114.2	116.6
MPW2PLYP	1.491	1.569	1.271	1.175	1.314	104.4	115.4	129.7	111.8	118.5
B2PLYP	1.496	1.536	1.283	1.156	1.389	105.7	114.6	128.3	108.8	122.9

Table 21. Mulliken charges at ethyl nitrate cation-radical atoms (e. u.)

Merhod	C^1	H^2	H^3	H^4	C^5	H^6	H^7	O^8	N^9	O^{10}	O^{11}
HF	–0.579	0.243	0.247	0.243	0.107	0.250	0.250	–0.579	1.627	–0.395	–0.414
MP2	–0.596	0.241	0.243	0.241	0.119	0.245	0.244	–0.491	1.389	–0.311	–0.325
PBEPBE	–0.497	0.221	0.224	0.228	0.117	0.269	0.227	–0.293	0.943	–0.232	–0.207
PW91PW91	–0.483	0.224	0.228	0.227	0.102	0.267	0.224	–0.285	0.940	–0.231	–0.212
OLYP	–0.417	0.189	0.188	0.183	0.273	0.179	0.230	–0.364	1.190	–0.343	–0.308
B3LYP	–0.491	0.225	0.242	0.233	0.062	0.214	0.246	–0.282	0.986	–0.228	–0.207
BHandHLYP	–0.583	0.231	0.237	0.231	0.100	0.242	0.242	–0.443	1.218	–0.380	–0.094
WB97XD	–0.606	0.238	0.244	0.238	0.039	0.246	0.246	–0.333	1.066	–0.287	–0.092
MPW2PLYP	–0.582	0.227	0.232	0.227	0.118	0.235	0.235	–0.389	1.019	–0.267	–0.054
B2PLYP	–0.574	0.230	0.236	0.230	0.113	0.240	0.240	–0.447	1.168	–0.352	–0.085

The ionization potential IP_v values as calculated according to Eq. (3) were in good agreement with the experimental data (Table 9). The largest deviation was observed in the case of BHandHLYP method (0.67 eV), whereas the average deviation was 0.43 eV.

The best agreement with the experiment in the case of ionization potential estimations according to the Koopmans theorem (IP_K, Table 21) was obtained in the cases of the BHandHLYP, wB97XD, MPW2PLYP, and B2PLYP methods, similarly to that observed in the cases of nitromethane and dimethylnitramine. Of those four methods, the smallest deviation from the experimental value was achieved in the wB97XD method (0.22 eV), whereas the average deviation for those methods was of 0.27 eV.

Thus, the presented results revealed that the OLYP and BHandHLYP methods could not be used in studies of ethyl nitrate anion-radical reactions. Note that the B3LYP, PBEPBE, PW91PW91, wB97XD, MPW2PLYP, and B2PLYP methods significantly overestimated the O–NO_2 bond length in the anion-radical, whereas the B3LYP, PBEPBE, PW91PW91, and OLYP methods overestimated the respective bond length in the cation-radical.

To conclude, the results of this work revealed some trends common for the cases of all studied compounds. The computed values of geometry parameters, dipole moments, and the vertical ionization potentials (3) were in agreement with the respective experimental data in the cases of neutral molecules. The ionization potential estimates made from the Koopmans theorem were in poorer agreement with the experiment; the ab initio methods significantly overestimated the ionization potential, while the DFT methods generally underestimated it. From the latter methods, the best results were achieved by using the wB97XD, mPW2PLYP, and B2PLYP methods. In computation of the adiabatic electron affinity, the best estimates for nitromethane were obtained with the wB97XD, BHandHLYP, mPW2PLYP, and B2PLYP methods.

In contrast with the neutral molecules, the geometry parameters of the studied ion-radicals strongly depend on employed method of quantum chemistry.

REFERENCES

1. Cottrell, T.L., Graham, T.E., and Reid, T.J., *Trans. Faraday Soc*., 1951, vol. 47, p. 1089.
2. Gray, P., Yoffe, A.D., and Roselaar, L., *Trans. Faraday Soc*., 1955, vol. 51, p. 1489.
3. Wilde, K.A., *Ind. Eng. Chem*., 1956, vol. 48, p. 769.
4. Smith, T.E. and Calvert, J.G., *J. Phys. Chem*., 1959, vol. 63, p. 1305.
5. Spokes, G.N. and Benson, S.W., *J. Am. Chem. Soc*., 1967, vol. 89, p. 2525.
6. Spokes, G.N. and Benson, S.W., *J. Am. Chem. Soc*., 1967, vol. 89, p. 6030.
7. Brill, T.B. and James, K.J., *Chem. Rev*., 1993, vol. 93, p. 2667.
8. Pola, J., Farkacova, M., Kubat, P., and Trka, A., *J. Chem. Soc*., 1984, vol. 80, p. 1499.
9. Shaw, R., *Int. J. Chem*., 1973, vol. 5, p. 261.
10. Nazin, G.M., Manelis, G.B., and Dubovitskii, D.I., *Russ. Chem. Rev*., 1968, vol. 37, p. 603.
11. Nazin, G.M., Manelis, G.B., and Dubovitskii, D.I., *Russ. Chem. Rev*., 1994, vol. 63, p. 313.
12. Nazin, G.M., Manelis, G.B., Rubtsov, Yu.I., and Strunin, V.A., *Thermal Decomposition and Combustion of Explosives and Propellants*, Boca Raton: CRC Press, 2003, p. 376.
13. Wodtke, A.M., Hintsa, E.J., and Lee, Y.T., *J. Phys. Chem*., 1986, vol. 90, p. 3549.
14. Shamsutdinov, A.F., Shamsutdinov, T.F., Shamov, A.G., and Khrapkovskii, G.M., *Int. J. Quantum Chem*., 2007, vol. 107, p. 2343.
15. Tsyshevsky, R.V., Aristov, I.V., Chachkov, D.V., Shamov, A.G., and Khrapkovskii, G.M., *J. Energ. Mater*., 2010, vol. 28, p. 318.
16. Khrapovskii, G.M., Shamov, A.G., Nikolaeva, E.V., and Chachkov, D.V., *Russ. Chem. Rev*., 2009, vol. 78, p. 903.
17. Sharia, O. and Kuklja, M.M., *J. Phys. Chem. (A),* 2010, vol. 114, p. 12656.
18. Denis, P.A., Ventura, O.N., Le, H.T., and Nguyen, M.T., *Phys. Chem. Chem. Phys*., 2003, vol. 5, p. 1730.
19. Manaa, M.R. and Fried, L.E., *J. Phys. Chem. (A)*, 1998, vol. 102, p. 9884.
20. Kiselev, V.G. and Gritsan, N.P., *J. Phys. Chem. (A)*, 2008, vol. 112, p. 4458.
21. Khrapovskii, G.M., Rozin, A.M., Tikhomirov, V.A., Shamov, A.G., and Marchenko, G.N., *Dokl. Akad. Nauk SSSR*, 1998, vol. 298, p. 921.
22. Bhattacharya, A., Guo, Yu., and Bernstein, E.R., *Acc. Chem. Res*., 2010, vol. 43, p. 1476.
23. Guo, Y.Q., Bhattacharya, A., and Bernstein, E.R., *J. Chem. Phys*., 2008, vol. 128, p. 034303.
24. Zijun Yu. and Bernstein, E.R., *J. Chem. Phys*., 2011, vol. 135, p. 154305.
25. Bhattacharya, A., Guo, Yu., and Bernstein, E.R., *J. Chem. Phys*., 2012, vol. 136, p. 024321.
26. Walker, I.C. and Fluendy, M.A.D., *Int. J. Mass Spectrometry*., 2001, vol. 205, p. 171.
27. Alizadeh, E., Ferreira da Silva 1, F., Zappa 2, F., Mauracher, A., Probst, M., Denifl, S., Bacher, A., Mark, T.D., Limao-Vieira 1, P., and Scheier, P., *Int. J. Mass Spectrometry*., 2008, vol. 271, p. 15.
28. Adamowicz, L., *J. Chem. Phys*., 1989, vol. 91, p. 7787.
29. Compton, R.N., Carman, H.S., Desfrancois, C., Abdoul-Carime, H., Schermann, J.P., Hendricks, J.H., Lyapustina, S.A., and Bowen, K.H., *J. Chem. Phys*., 1996, vol. 105, p. 3472.
30. Gutsev, G.L. and Bartlett, R.J., *J. Chem. Phys*., 1996, vol. 105, p. 8785.
31. Arenas, J.F., Otero, J.C., Pelaez, D., Soto, J., and Serrano-Andres, L., *J. Chem. Phys*., 2004, vol. 121, p. 4127.
32. Sailer, W., Pelc, A., Matejcik, S., Illenberger, E., Scheier, P., and Mark, T.D., *J. Chem. Phys*., 2002, vol. 117, p. 7989.
33. Edtbauer, A., Sulzer, P., Mauracher, A., Mitterdorfer, C., Ferreira da Silva, F., Denifl, S., Mark, T.D., Probst, M., Nunes, Y., Limao-Vieira, P., and Scheier, P., *J. Chem. Phys*., 2010, vol. 132, p. 134305.
34. Sulzer, P., Mauracher, A., Denifl, S., Zappa, F., Ptasinska, S., Beikircher, M., Bacher, A., Wendt, N., Aleem, A., Rondino, F., Matejcik, S., Probst, M., Mark, T.D., Scheier, P., *Anal. Chem*., 2007, vol. 79, p. 6585.
35. Sulzer, P., Mauracher, A., Denifl, S., Probst, M., Mark, T.D., Scheier, P., and Illenberger, E., *Int. J. Mass Spectrometry.*, 2007, vol. 266, p. 138.

36. Sulzer, P., Mauracher, A., Ferreira da Silva, F., Denifl, S., Mark, T.D., Probst, M., Limao-Vieira, P., and Scheier, P., *J. Chem. Phys*., 2009, vol. 131, p. 144304.
37. Sulzer, P., Rondino, F., Ptasinska, S., Illenberger, E., Mark, T.D., and Scheier, P., *Int. J. Mass Spectrometry*., 2008, vol. 272, p. 149.
38. Aluker, E.D., Krechetov, A.G., Mitrofanov, A.Yu., Nurmukhame-tov, D.R., and Kuklja, M.M., *J. Phys. Chem*., 2011, vol. 115, p. 6893.
39. Ewing, R.G., Atkinson, D.A., Eiceman, G.A., and Ewing, G.J., *Talanta*, 2001, vol. 54, p. 515.
40. Walsh, M.E., *Talanta*, 2001, vol. 54, p. 427.
41. Nikolaeva, E.V., *Candidate Sci. (Chem.) Dissertation*, Kazan, 2002
42. Tsyshevskuu, R.V. *Candidate Sci. (Chem.) Dissertation*, Kazan, 2008.
43 Khrapovskii, G.M., Chachkov, D.V., Nikolaeva, E.V., and Shamov, A.G., *Vest. Kazan. Tekh. Univ*., 2011, vol. 20, p. 55.
44. Tsyshevsky, R.V., Garifzianova, G.G., Chachkov, D.V., Shamov, A.G., and Khrapkovskii, G.M., *J. Energ. Mater*., 2009, vol. 27, P. 263.
45. Sharipov, D.D., Egorov, D.L., Chachkov, D.V., Shamov, A.G., and Khrapkovskii, G.M., *Russ., J. Gen. Chem.*, 2011, vol. 81, no. 11, p. 2273.
46. Garivzianova, G.G., Tsyshevsky, R.V., Shamov, A.G., and Khrapkovskii, G.M., *Int. J. Quantum Chem*., 2007, vol. 107, p. 2489.
47. Olivella, S., Sole Al., McAdoo, D.J., and Griffins, L.L., *J. Am. Chem. Soc*., 1994, vol. 116, p. 11078.
48. Moller, C. and Plesset, M.S., *Phys. Rev*., 1934, vol. 46, p. 0618.
49. Perdew, J.P., Burke, K., and Ernzerhof, M., *Phys. Rev. Lett*., 1996, vol. 77, p. 3865.
50. Perdew, J.P., Burke, K., and Ernzerhof, M., *Phys. Rev. Lett*., 1996, vol. 77, p. 3865.
51. Perdew, J.P., Chevary, J.A., Vosko, S.H., Jackson, K.A., Pederson, M.R., Singh, D.J., and Fiolhais, C., *Phys. Rev*., 1992, vol. 46, p. 6671.
52. Perdew, J.P., Burke, K., and Wang, Y., *Phys. Rev*., 1996, vol. 54, p. 16533.
53. Handy, N.C. and Cohen, A.J., *Mol. Phys*., 2001, vol. 9, p. 403-12.
54. Lee, C., Yang, W., and Parr, R.G., *Phys. Rev*., 1988, vol. 37, p. 785.
55. Becke, A.D., *J. Chem. Phys*., 1993, vol. 98, p. 5648.
56. Becke, A.D., *J. Chem. Phys*., 1993, vol. 98, p. 1372.
57. Grimme, S., *J. Chem. Phys*., 2006, vol. 124, p. 034108.
58. Schwabe, T. and Grimme, S., *Phys. Chem. Chem. Phys*., 2006, vol. 8, p. 4398.
59. Hohenberg, P. and Kohn, W., *Phys. Rev. (B).,* 1964, vol. 136, p. 864.
60. Kohn, W. and Sham, L.J., *Phys. Rev. (A).,* 1965, vol. 140, p. 1133.
61. Chai, J.D. and Head-Gordon, M., *Phys. Chem. Chem. Phys*., 2008, vol. 10, p. 6615.
62. Chai, J.D. and Head-Gordon, M., *J. Chem. Phys*., 2008, vol. 128, p. 084106.
63. Frisch, M.J., Trucks, G.W., Schlegel, H.B., Scuseria, G.E., Robb, M.A., Cheeseman, J.R., Scalmani, G., Barone, V., Mennucci, B., Petersson, G.A., Nakatsuji, H., Caricato, M., Li, X., Hratchian, H.P., Izmaylov, A.F., Bloino, J., Zheng, G., Sonnen-berg, J.L., Hada, M., Ehara, M., Toyota, K., Fukuda, R., Hasegawa, J., Ishida, M., Nakajima, T., Honda, Y., Kitao, O., Nakai, H., Vreven, T., Montgomery, J.A., Jr., Peralta, J.E., Ogliaro, F., Bearpark, M., Heyd, J.J., Brothers, E., Kudin, K.N., Staroverov, V.N., Kobayashi, R., Normand, J., Raghavachari, K., Rendell, A., Burant, J.C., Iyengar, S.S., Tomasi, J., Cossi, M., Rega, N., Millam, J.M., Klene, M., Knox, J.E., Cross, J.B., Bakken, V., Adamo, C., Jaramillo, J., Gomperts, R., Stratmann, R.E., Yazyev, O., Austin, A.J., Cammi, R., Pomelli, C., Ochterski, J.W., Martin, R.L., Morokuma, K., Zakrzewski, V.G., Voth, G.A., Salvador, P., Dannenberg, J.J., Dapprich, S., Daniels, A.D., Farkas, O., Foresman, J.B., Ortiz, J.V., Cioslowski, J., and Fox, D.J., *GAUSSIAN 09*, Rev. A.1, Gaussian, Inc., Wallingford CT, 2009.
64. Taylor, W.D., Allston, T.D., Moscato, M.J., Fazekas, G.B., Kozlowski, R., and Takacs, G.A., *Int. J. Chem. Kinet*., 1980, vol. 12, p. 231.
65. *NIST Computational Chemistry Comparison and Benchmark Database*, NIST Standard Reference Database Number 101, Rel. 15b.
66. *Landolt-Bornstein. Group II: Atomic and Molecular Physics,* Hellwege, K.H. and Hellwege, A.M., Eds., Berlin: Springer–Verlag, 1976, vol. 7.
67. George, M.V. and Wright, G.F., *J. Am. Chem. Soc*., 1958, vol. 80, p. 1200.
68. Mulliken, R.S., *J. Chem. Phys*., 1955, vol. 23, no. 10, p. 1833.
69. Sumpter, B.G. and Thompson, D.L., *J. Chem. Phys*., 1998, vol. 88, p. 6889.
70. Nigenda, E., McMillen, D.F., and Golden, D.M., *J. Phys. Chem*., 1989, vol. 93, p. 1124.
71. Flournoy, J.M., *J. Chem. Phys*., 1962, vol. 36, p. 1106.
72. Harris, N.J. and Lammertsma, K., *J. Phys. Chem*. (*A).,* 1997, vol. 101, no. 7, p. 1370.
73. Oxley, J.C., Hiskey, M., Naud, D., and Szekeres, R., *J. Phys. Chem*., 1992, vol. 96, no. 6, p. 2505.
74. Velardez, G.F., Alavi, S., and Thompson, D.L., *J. Chem. Phys*., 2005, vol. 123, p. 074313.
75. Johnson, M.A. and Truong, T.N., *J. Phys. Chem*., 1999, vol. 103, p. 9392.